ASM Sc. J., 14, Special Issue 1, 2021 for ICSTSS2018, 148-154

Electrochemical Performance of Electrodeposited Ni/GDC Anodes for Solid Oxide Fuel Cells

Zadariana Jamil[1]*, Enrique Ruiz-Trejo[2] and Nigel P Brandon[2]

[1]*School of Civil Engineering, College of Engineering, Universiti Teknologi MARA, 40450 Shah Alam, Selangor, Malaysia*

[2]*Department of Earth Science and Engineering, Imperial College London, SW7 2AZ, United Kingdom*

The fabrication of SOFC anodes using infiltration method has shown a potential to produce an excellent anode performance with a relatively reduced amount of nickel. Nonetheless, infiltration method is very challenging for industrial application due to its lengthy and energy consuming process, which involves repeated Ni nitrate solution infiltration, heating and cooling cycles. A combination of electroless and electrodeposition technique has shown a promising alternative method due to its ability to accelerate the Ni adding process into porous scaffolds at near-room or room temperature. Ni loadings range between ~5 to ~18 vol% were deposited onto the GDC scaffolds to demonstrate the catalytic role of Ni loadings on the electrochemical performance of the electrodeposited anodes. The total electrode polarisation of the anodes exhibited a promising result when the loading of Ni 5.3 vol% (0.74 Ω.cm^2). Further, increases in Ni loadings to 17.6 vol% Ni, relatively decreased the performance of the electrode to 1.25 Ω.cm^2.

Keywords: anodes; electrodeposition; electroless; electrochemical performance; solid oxide fuel cells

I. INTRODUCTION

Ni-$Ce_{0.9}Gd_{0.1}O_{1.95}$ (Ni/GDC) ceramic-metal composites (cermets) are widely used as solid oxide fuel cell anodes due to their ability to electrochemically oxidise different types of fuels such as H_2, methane, ethanol and H_2S. However, the use of these fuels (other than H_2) may deposit impurities on the cells such as carbon and sulfur, which may degrade the SOFC performance (Offer *et. al.*, 2009; Chen *et al.*, 2016). Several research groups have experimentally shown that Ni/GDC-based anodes are tolerance to sulfur poisoning (Riegraf *et al.*, 2018) and carbon deposition (Marina *et. al.*, 1999; Liu *et. al.*, 2013; Augusto *et al.*, 2014). This shows that Ni/GDC is a promising SOFC anode due to its full reversibility of the poisoning and lower performance drop.

Ni performs as a catalyst for fuel oxidation and electronic conductor. GDC is a mixed ionic and electronic conductor in reducing atmospheres at high temperature (Nakamura *et al.*, 2008). Thus, the use of GDC as an SOFC anode component provides high surface activity towards hydrogen oxidation, which takes place at triple-phase boundary (TPB) and extends to double phase boundary (DPB). TPB is the area where the gas phase, ionic conductor and electronic conductor meet, whereas DPB is the area where the gas and mixed ionic and electronic conductor meet. These meeting points are the electrochemical reaction sites, where electrons are released and produce electricity.

A successful anode cermet highly depends on the materials, that should exhibit a high catalytic activity for the desired chemical and electrochemical reactions, chemical stability with the reaction atmospheres and chemical compatibility with other components. Furthermore, the microstructure of the anodes should display a large number of reaction sites. Thus, fabrication methods of the anodes are closely related to design the required anode microstructures with high electrochemical performance.

*Corresponding author's e-mail: riana_jay@yahoo.com.sg

The most common SOFC anode fabrication methods are powder mixing and impregnation. The powder mixing method (i) requires a large Ni volume (>30 vol%) to achieve acceptable electronic conductivity and electrochemical performance (Macedo *et al.*, 2013); (ii) involves high sintering temperatures to form the required material microstructures, which can introduce to a large amount of undesirable defects such as crack during processing and operation due to mismatch and shrinkage of the materials and (iii) prevents the incorporation of low melting point metal catalysts such as Cu into the anodes. The impregnation method overcomes the limitations in powder mixing method by separately sintering ionic conductor scaffold at high temperatures and incorporating metal catalyst (Futamura *et al.*, 2017). This method also allows the formation of nano-sized metal and oxide particles that will increase the TPBs. The disadvantage of this method is lengthy process due to its multiple infiltration, heating and cooling steps to achieve satisfactory electronic conductivity throughout the electrode (at least 10 successive metal impregnations) (Lomberg *et al.*, 2014). Thus, it is costly and may not be suitable for large production.

Previously we have introduced a new route for anode fabrication by combining electroless and electrode processes (Ruiz-Trejo *et. al.*, 2015; Jamil *et al.*, 2016). This method has shown promising results by fabricating the anodes using simple steps and techniques, hence, potentially used for mass production. In this paper we presented the effect of Ni content on the electrochemical performance of the anode using this method. We fabricated Ni/GDC anodes using electroless and electrodeposition method at different percentage of Ni (0, 5 and 18 %vol) and their performance and behaviour were investigated.

II. MATERIALS AND METHOD

A. Preparation of Symmetrical Cells

The details fabrication of electrodeposited symmetrical cells (Ni/Ag/GDC|YSZ|Ni/Ag/GDC) were fabricated and described by Jamil *et al.* (2016). The GDC ink was prepared by mixing GDC powder (Fuel Cell Materials), carbon and solvents as described in Figure 1. Then, the GDC ink was screen printing symmetrically on yttria-stabilised zirconia (YSZ) electrolytes on both sides and then sintered at 1300 °C in air for 1 hour, forming GDC scaffolds. Ag layer was first deposited on the GDC scaffolds and Ni was then electrodeposited using Watts bath on the Ag layer. The electroless and electrodeposition process is described in details by Jamil *et al.* (2017) and summarised in Figure 2.

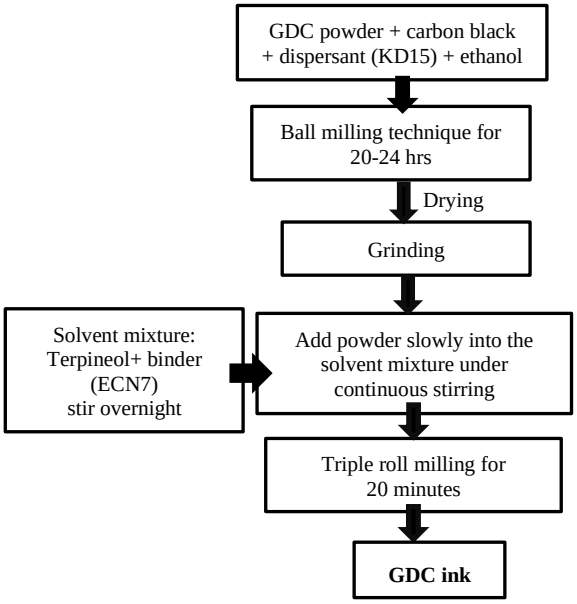

Figure 1. Steps of GDC ink preparation

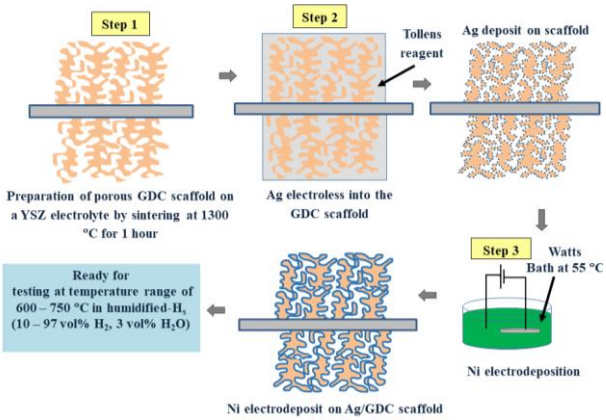

Figure 2. Summary of metallising process of GDC scaffolds

B. Symmetrical Cells Measurement

The performance of symmetrical cells (Table 1) was measured using a potentiostat (Autolab PGSTAT302N). The electrochemical impedance spectroscopy (EIS) of the symmetrical cells were done in a four-electrode system in the frequency range of 10^{-1} – 10^{5} Hz using an AC signal amplitude of 20 mV. All the tests were done in humidified-H_2 (10 – 97 vol% H_2, 3 vol% H_2O) at 600 – 750 °C.

Table 1. The symmetrical cells composition prepared in this study

Electrode sample	Electrode composition (vol%)
Z001: (Ag/GDC)	18.9/81.1
Z002: (Ni/Ag/GDC)	5.3/35.3/59.4
Z003: (Ni/Ag/GDC)	17.6/22.2/59.8

C. Microstructures Characterisation

The microstructure of symmetrical cells after testing were analysed using scanning electron microscopy (SEM; LEO Gemini 1525 FEGSEM) and electron-dispersive X-ray spectroscopy (EDX; JEOL-6400).

III. RESULTS AND DISCUSSION

Figure 3 (a) top and (b) cross section views of GDC scaffold after sintering process at 1300 °C for 1 hr shows the GDC scaffolds prepared in this study. The porosity of the GDC scaffold ~70 vol%. The porosity of the scaffold was calculated by comparing the theoretical GDC density (7.21 g.cm^{-3}) and the experimental density (obtained from mass and volume of the scaffold) (Jamil *et al.*, 2016). Pores with larger size are required to assist the deposition of Ag and Ni within the scaffold, by allowing the penetration of Tollens' and Watts solutions into a greater depth of the scaffold, respectively. Figure 4 shows the metallised GDC scaffold before testing. Ag deposits covered the GDC scaffold (Figure 4(a)) and made it electronically conductive, enabling Ni deposition onto the Ag/GDC scaffold (Figure 4(b)). It is evident isolated Ag islands formed on the top of the electrode, associated with the movement of Ag in an upward direction to the electrode surface when heated to high temperatures in reduced atmospheres (Figure 5). It is evident that Ag layer agglomerates when temperature increases to > 250 °C (Proux *et. al.*, 1999; Kawamura *et. al.*, 2005; Sholklapper *et al.*, 2008). This allows the contact of Ni and GDC and forms TPB sites for electrochemical reactions. The formation of Ag on the top of the electrode serves as a current collector as there was no additional Ag paste used to connect the platinum mesh to the measuring cell. Ag did not serve as a catalyst in this anode other than providing electrically conductive layer for Ni electrodeposition.

The electrochemical performance of the electrodeposited symmetrical cells with Ni content of 0 (Z001), 5.3 (Z002) and 17.6 vol% (Z003) was measured using impedance measurements over the temperature range of 600 - 750 °C in 20 – 100 vol% humidified H_2 (balance gas was N_2 and the humidity ~3 vol% H_2O). Most of the spectra consist of two of semicircles, at intermediate (10 – 10^3 Hz) and low (<10) frequencies, linked to intermediate-frequency (*R_m)* and low-frequency (*R_l*) polarisations, respectively (Figure 6) The ohmic resistance (R_{ohm}) is obtained from the intercept of the real (Z') axis with the impedance spectra at high frequency. The polarisation resistance values for the symmetrical cells were approximated by fitting the impedance data to the equivalent electrical circuit shown in Figure 7, and then the extracted values were normalised by dividing by two and multiplying by the area of the electrode (1.368 cm^2).

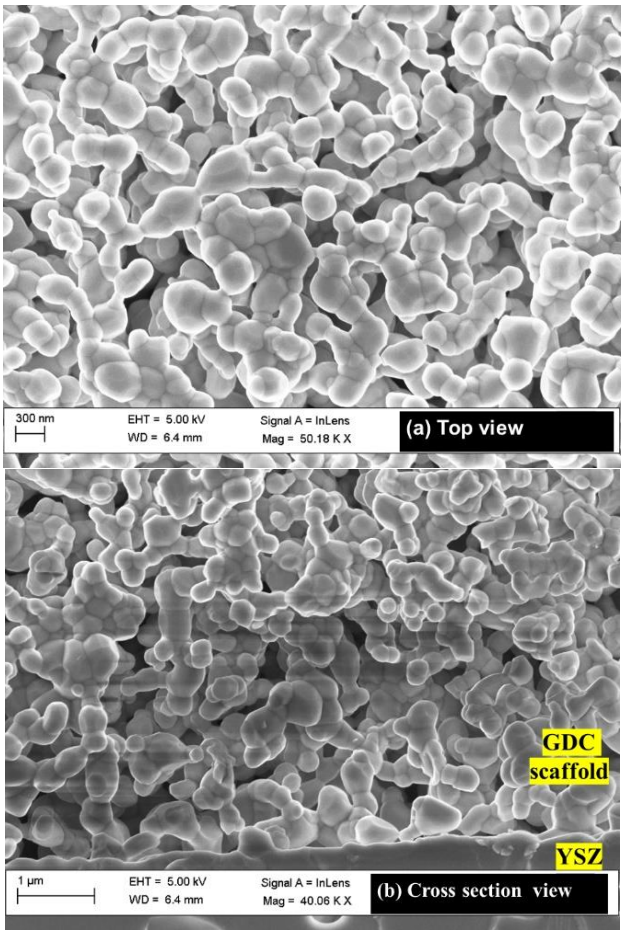

Figure 3. (a) Top and (b) cross section views of GDC scaffold after sintering process at 1300 °C for 1 hr

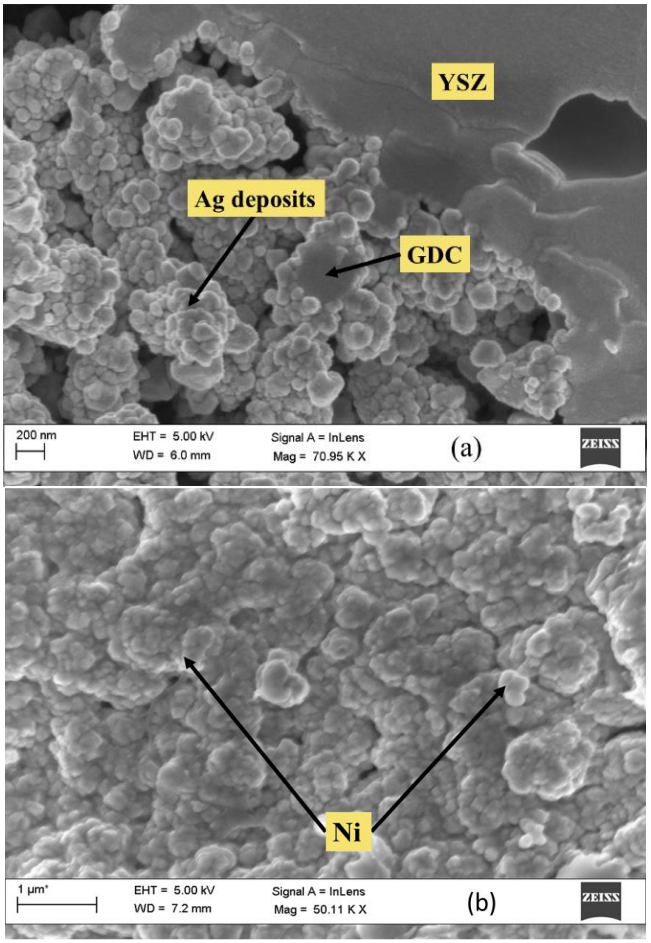

Figure 4. The GDC scaffold (a) after Ag deposition using Tollens reaction and (b) after Ni electrodeposition using Watts solution

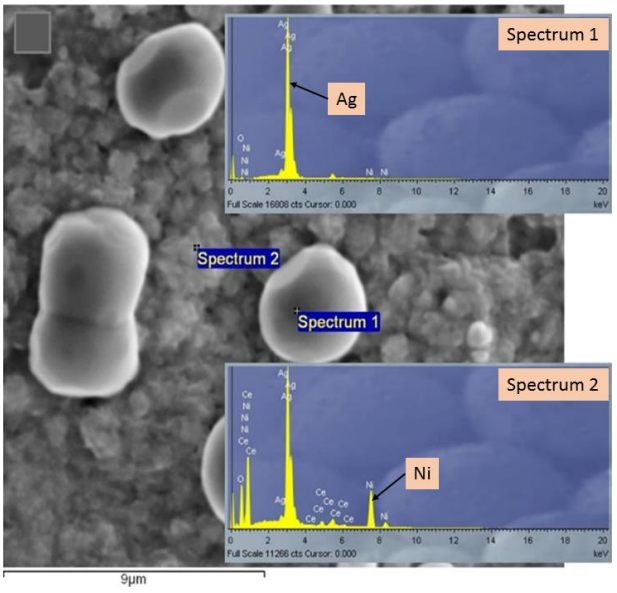

Figure 5. Microstructural changes of metallised GDC scaffold after reduction process at 600 °C. The graphs are the elemental analysis for the electrode.

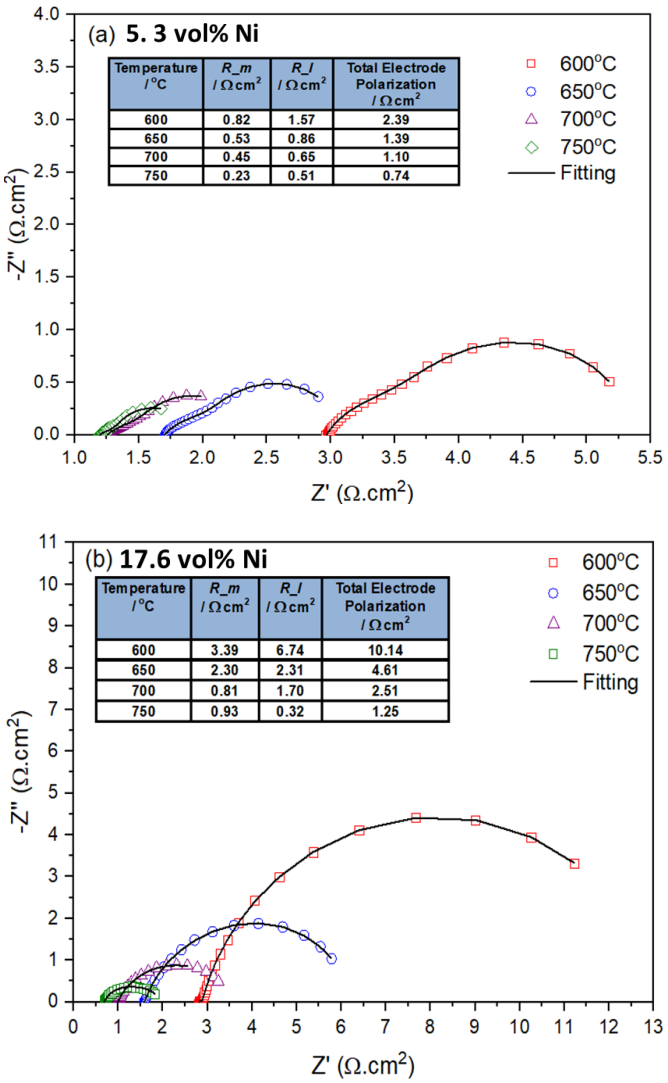

Figure 6. Impedance spectra symmetrical cells (a) Z002 (5.3 vol% Ni) and (b) Z003 (17.6 vol %) at temperatures range from 600 to 750 °C in humidified H_2 (97%H_2 – 3%H_2O) in the frequency range of 0.1-10^5 Hz. The inset tables present the list of polarisation resistance of the electrodes at different temperature.

Figure 6 shows R_{ohm} of both symmetrical cells, Z002 and Z003 decreasing when the temperature increases to 750 °C. This is expected as the R_{ohm} is linked to the ionic conductivity of the YSZ electrolyte, which is thermally activated, together with marginal contributions from the electrode and contact resistance (Macedo *et al.*, 2014). The total electrode polarisation or area specific resistance (ASR) is the total sum of R_m and R_l, indicating the electrochemical performance of the electrode. Both R_m and R_l are associated with the anode polarisation resistance, which are generally related to charge transfer and gas diffusional processes, respectively (Monzon *et. al.*,

2014; López-Robledo *et al.*, 2015).

Figure 6 shows the ASR, *R_m* and *R_l* values of Z002 and Z003 decreased by ~70 % with increasing temperature from 600 to 750 °C, indicating a clear enhancement on the electrochemical performance of the anodes due to thermal activation (Macedo *et al.*, 2014). The ASR values, which characterise the electrochemical performance of the electrodes, are summarised in the inset tables in Figure 6. The lowest ASR was 0.74 Ω.cm² and achieved with 5.3 vol% of Ni (Z002) at 750 °C in humidified H_2 (97%H_2 – 3%H_2O). The ASR of the electrode increased to 1.25 Ω.cm² when Ni loadings were increased to 17.6 vol%. It was expected that the performance of the electrode would improve as the total ASR would decrease by the increase of Ni content due to improvement of electronic conducting pathways throughout the electrode (Li *et al.*, 2011). It is also shown that the *R_m* of Z003 (0.93 Ω.cm²) was three times greater than the *R_l* (0.32 Ω.cm²), most likely associated with the delamination of anode/electrolyte interface (Figure 8), where the charge transfer process occurs (Smith *et. al.*, 2009; Nerat and Juricic, 2018). The delamination may be caused by the migration, segregation and agglomeration of both metals (Ni and Ag) in reducing atmospheres and at high temperatures that may affect the anode structure (Muecke *et al.*, 2008).

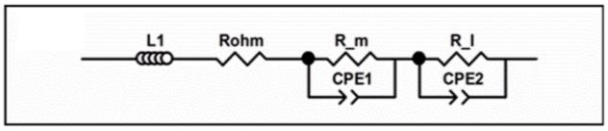

Figure 7. The electrical circuit used for data fitting in this study

The values of ASR with and without Ni are summarised in Figure 9. A decrease in total ASR was observed when small amount of Ni (5.3 vol%) was added, hence the performance of the electrode improved. This shows the role of Ni as the catalyst of electrochemical reactions at the SOFC anodes, although in small amounts of Ni (Wang *et al.*, 2009). Furthermore, the mixed ionic-electronic conducting properties of GDC also play an important role, as the reaction zone extends to the two-phase interface of GDC electrode/gas via chemical diffusion through the electrode (Primdahl & Mogensen, 2002). Thus, the electrode reaction sites may extend from TPBs to double phase boundaries (DPBs). Further investigation is needed to obtain the optimum Ni can be electrodeposited into Ag/GDC scaffolds, thus, may improve the electrochemical performance of the electrodeposited Ni/Ag/GDC anodes.

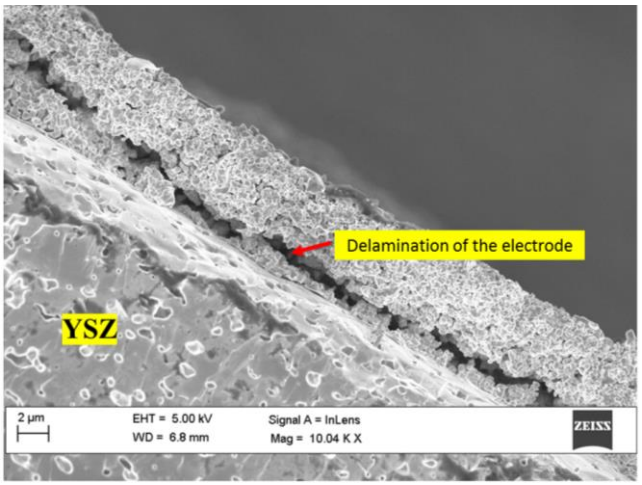

Figure 8. The SEM image of Z003 after being tested at 750 °C in humidified H_2. The Ni/Ag/GDC anode delaminated from YSZ electrolyte.

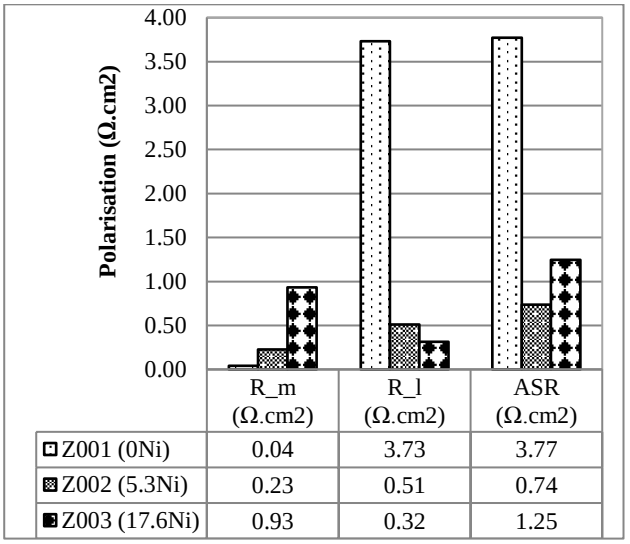

	R_m (Ω.cm2)	R_l (Ω.cm2)	ASR (Ω.cm2)
Z001 (0Ni)	0.04	3.73	3.77
Z002 (5.3Ni)	0.23	0.51	0.74
Z003 (17.6Ni)	0.93	0.32	1.25

Figure 9. Summary of electrochemical performance of electrodeposited Ni/Ag/GDC (Z002 AND Z003) and Ag/GDC (Z001) electrodes operating at OCV and 750°C in humidified H_2.

IV. CONCLUSION

The electrochemical performance of the electrodeposited anodes significantly improved when small amount of Ni was added into the anodes. However, further addition of Ni to 17.6 vol% caused the delamination of the anode/electrolyte interface, thus, decreased the performance of the anodes.

V. ACKNOWLEDGEMENT

The authors would like to acknowledge UiTM Slab, Ministry of Education Malaysia Scholarship and EPSRC through project "Advancing Biogas Utilization through Fuel Flexible SOFC" for funding this work. Also UiTM Pahang for partially funding ICSTSS 2018 fee.

VI. REFERENCES

Augusto, BL, Noronha, FB, Fonseca, FC, Tabuti, FN, Colman, RC & Mattos, LV 2014, 'Nickel/gadolinium-doped ceria anode for direct ethanol solid oxide fuel cell', International Journal of Hydrogen Energy, vol. 39, no. 21, pp. 11196–11209. doi: 10.1016/j.ijhydene.2014.05.088.

Chen, H, Wang, F, Wang, W, Chen, D, Li, S-D & Shao, Z 2016 'H2S poisoning effect and ways to improve sulfur tolerance of nickel cermet anodes operating on carbonaceous fuels', Applied Energy, vol. 179, no. 5, pp. 765–777. doi: 10.1016/j.apenergy.2016.07.028.

Futamura, S, Tachikawa, Y, Matsuda, J, Lyth, SM, Shiratori, Y, Taniguchi, S & Sasaki, K 2017, 'Alternative Ni-impregnated mixed ionic-electronic conducting anode for SOFC operation at high fuel utilisation', Journal of the Electrochemical Society, vol. 164, no. 10, pp. 3055–3063. doi: 10.1149/2.0071710jes.

Jamil, Z, Ruiz-Trejo, E, Boldrin, P & Brandon, NP 2016, 'Anode fabrication for solid oxide fuel cells: electroless and electrodeposition of nickel and silver into doped ceria scaffolds', International Journal of Hydrogen Energy, vol. 41, no. 22, pp. 9627–9637. doi: 10.1016/j.ijhydene.2016.04.061.

Kawamura, M, Yamaguchi, M, Abe, Y & Sasaki, K 2005, 'Electrical and morphological change of Ag-Ni films by annealing in vacuum', Microelectronic Engineering, vol. 82, no. 3–4, pp. 277–282. doi: 10.1016/j.mee.2005.07.035.

Li, L, Zhang, P, Liu, R & Guo, SM 2011, 'Preparation of fibrous Ni-coated-YSZ anodes for solid oxide fuel cells', Journal of Power Sources, vol. 196, no. 3, pp. 1242–1247. doi: 10.1016/j.jpowsour.2010.08.038.

Liu, M 2013, van der Kleij a, Verkooijen a, HM, Aravind, PV, 'An experimental study of the interaction between tar and SOFCs with Ni/GDC anodes', Applied Energy, vol. 108, pp. 149–157. doi: 10.1016/j.apenergy.2013.03.020.

López-Robledo, MJ, Laguna-Berceco, MA, Dilve, J, Orera, VM & Larrea, A 2015, 'Electrochemical performance of intermediate temperature micro-tubular solid oxide fuel cells using porous ceria barrier layers', Ceramics International, vol. 41 no. 6, pp. 7651–7660. doi: 10.1016/j.ceramint.2015.02.093.

Macedo, DA, Souza, GL, Cela, B, Paskocimas, CA, Martinelli, AE, Figueiredo, FM, Marques, FM & Nascimento, RM 2013 'A versatile route for the preparation of Ni-CGO cermets from nanocomposite powders', Ceramics International, vol. 39, no. 4, pp. 4321–4328. doi: 10.1016/j.ceramint.2012.11.014.

Macedo, DA, Figueiredo, FML, Paskocimas, CA, Martinelli, AE, Nascimento, RM, & Marques, FMB 2014 'Ni–CGO cermet anodes from nanocomposite powders: microstructural and electrochemical assessment', Ceramics International, vol. 40, no. 8, pp. 13105–13113. doi: 10.1016/j.ceramint.2014.05.010.

Marina, OA, BAgger, C, Primdahl, S & Morgensen, M 1999, 'A solid oxide fuel cell with a gadolinia-doped ceria anode: preparation and performance', Solid State Ionics, vol. 123, pp. 199–208. doi: 10.1016/S0167-2738(99)00111-3.

Monzon, H, Laguna-Bercero, MA, Larrea, A, Arias, BI, Varez, A & Levenfeld, B 2014, 'Design of industrially scalable microtubular solid oxide fuel cells based on an extruded support', International Journal of Hydrogen Energy, vol. 39, pp. 5470–5476. doi: 10.1016/j.ijhydene.2014.01.010.

Muecke, UP, Graf, S, Rhyner, U & Gauckler, LJ 2008, 'Microstructure and electrical conductivity of nanocrystalline nickel- and nickel oxide/gadolinia-doped ceria thin films', Acta Materialia, vol. 56, no. 4, pp. 677–687. doi: 10.1016/j.actamat.2007.09.023.

Nerat, M & Juricic, D 2018, 'Modelling of anode delamination in solid oxide electrolysis cell and analysis of its effects on electrochemical performance', International Journal of Hydrogen Energy, vol. 43, no. 17, pp. 8179–8189. doi: org/10.1016/j.ijhydene.2018.02.189

Offer, GJ, Brightman, E & Brandon, NP 2009, 'Thermodynamics and kinetics of the interaction of carbon and sulfur with solid oxide fuel cell anodes', Journal of the American Ceramic Society, vol. 92, no. 4, pp. 763–780. doi: 10.1111/j.1551-2916.2009.02980.x.

Proux, O, Revenant-Brizard, C, Regnard, JR & Mevel, B 1999, 'Structural evolution of NiAg heterogeneous alloys upon annealing', Journal of Physics: Condensed Matter, vol. 11, pp. 147–162. iopscience.iop: 0953-8984/11/1/013.

Riegraf, M, Zekri, A, Knipper, M, Costa, R, Schiller, G & Friedrich, KA 2018, 'Sulfur poisoning of Ni/Gadolinium-doped ceria anodes: a long-term study outlining stable solid oxide fuel cell operation', Journal of Power Sources, vol. 380, pp. 26–36. doi: 10.1016/j.jpowsour.2018.01.067.

Ruiz-Trejo, E, Atkinson, A, & Brandon, NP 2015, 'Metallizing porous scaffolds as an alternative fabrication method for solid oxide fuel cell anodes', Journal of Power Sources, vol. 280, pp. 81–89. doi: 10.1016/j.jpowsour.2015.01.091.

Sholklapper, TZ, Radmlovic, V, Jacobson, CP, Visco, SJ & De Jonghe, LC 2008, 'Nanocomposite Ag-LSM solid oxide fuel cell electrodes', Journal of Power Sources, vol. 175, no. 1, pp. 206–210. doi: 10.1016/j.jpowsour.2007.09.051.

Smith, JR, Chen, A, Gostovic, D, Hickey, D, Kundinger, D, Duncan, KL, DeHoff, RT, Jones, KS & Wachsman, ED 2009, 'Evaluation of the relationship between cathode microstructure and electrochemical behavior for SOFCs', Solid State Ionics, vol. 180, pp. 90–98. doi: 10.1016/j.ssi.2008.10.017.